
Unsupervised Regionalization of Particle-resolved Aerosol Mixing State Indices on the Global Scale

Zhonghua Zheng

Department of Civil and Environmental Engineering
University of Illinois at Urbana-Champaign
Urbana, IL 61801
zzheng25@illinois.edu

Joseph Ching

Meteorological Research Institute
Japan Meteorological Agency
1-1 Nagamine, Tsukuba, Ibaraki, 305-0052, Japan.
jching@mri-jma.go.jp

Jeffrey H. Curtis

Department of Mechanical Science and Engineering
University of Illinois at Urbana-Champaign
Urbana, IL 61801
jcurtis2@illinois.edu

Yu Yao

Department of Atmospheric Sciences
University of Illinois at Urbana-Champaign
Urbana, IL 61801
yuyao3@illinois.edu

Peng Xu

School of Environmental Science and Engineering
Southern University of Science and Technology
Shenzhen 518055, Guangdong Province, China
xup@sustech.edu.cn

Matthew West

Department of Mechanical Science and Engineering
University of Illinois at Urbana-Champaign
Urbana, IL 61801
mwest@illinois.edu

Nicole Riemer

Department of Atmospheric Sciences
University of Illinois at Urbana-Champaign
Urbana, IL 61801
nriemer@illinois.edu

Abstract

The aerosol mixing state significantly affects the climate and health impacts of atmospheric aerosol particles. Simplified aerosol mixing state assumptions, common in Earth System models, can introduce errors in the prediction of these aerosol impacts. The aerosol mixing state index, a metric to quantify aerosol mixing state, is a convenient measure for quantifying these errors. Global estimates of aerosol mixing state indices have recently become available via supervised learning models, but require regionalization to ease spatiotemporal analysis. Here we developed a simple but effective unsupervised learning approach to regionalize predictions of global aerosol mixing state indices. We used the monthly average of aerosol mixing state indices global distribution as the input data. Grid cells were then clustered into regions by the k -means algorithm without explicit spatial information as input. This approach resulted in eleven regions over the globe with specific spatial aggregation patterns. Each region exhibited a unique distribution of mixing state indices and aerosol compositions, showing the effectiveness of the unsupervised regionalization approach. This study defines “aerosol mixing state zones” that could be useful for atmospheric science research.

1 Introduction and Motivation

The concept of aerosol mixing state describes how different aerosol chemical species are distributed among the particles in a population [Riemer et al., 2019]. A completely “externally mixed” population contains only one species per particle, while a completely “internally mixed” population contains particles with the same composition as the bulk population. Many different intermediate mixing states are possible between those two extremes, and these commonly occur in the ambient atmosphere. Aerosol mixing state influences the particles’ properties such as hygroscopicity [Fierce et al., 2017, Holmgren et al., 2014], optical properties [Fierce et al., 2016, Jacobson, 2001], cloud condensation nuclei activity [Ching et al., 2012, Wang et al., 2010], ice nucleation potential [Knopf et al., 2018], the aerosols’ lifetime [Koch et al., 2009] in the atmosphere, and their deposition in the human respiratory system [Ching and Kajino, 2018]. However, Earth System models (ESMs) or regional climate models usually hold simplified mixing state assumptions. These can influence how accurately physicochemical properties of aerosols are predicted [Ching and Kajino, 2018, Fierce et al., 2017], and thereby limit the accuracy of estimating aerosol impacts on climate and health.

Riemer and West [2013] proposed an entropy-based diversity metric to quantify aerosol mixing state. This metric, the mixing state index (χ), has a range from 0% (a fully externally mixed population) to 100% (a fully internally mixed population). The index χ has been applied to both modeling [Zhu et al., 2016] and experimental [Healy et al., 2014, O’Brien et al., 2015, Fraund et al., 2017, Bondy et al., 2018, Ye et al., 2018] work. For example, χ has been used for quantifying errors in CCN concentration [Ching et al., 2017] prediction, as well as the prediction of soot particles depositing in the human respiratory system [Ching and Kajino, 2018].

Knowing the global distribution of aerosol mixing state index is desirable, as it can be used for error quantification at the large scale. But deriving this distribution directly by using a benchmarking particle-resolved model [Riemer et al., 2009] at the global scale would be computationally prohibitive over the time scales of interest. To overcome this limitation, supervised-learning emulators were developed for predicting the spatial distribution aerosol mixing state across the globe [Hughes et al., 2018, Zheng et al., 2020]. However, the spatial delimitation based on aerosol mixing state indices remains unclear, which hinders further spatiotemporal analysis.

The research questions for this paper are: (1) Is it possible to regionalize the global mixing state indices, i.e., define aerosol mixing state zones, similar to distinct climate zones [Fovell and Fovell, 1993, Mitchell, 1976]? (2) What are spatiotemporal patterns of the regionalized mixing state indices? This paper describes an effort to regionalize the global mixing state indices using a simple but effective unsupervised learning approach.

2 Methods

2.1 Mixing state indices definition

The mixing state index χ [Riemer and West, 2013] is given by the affine ratio of the average particle species diversity (D_α) and bulk population species diversity (D_γ) as $\chi = \frac{D_\alpha - 1}{D_\gamma - 1}$. The diversities D_α and D_γ are calculated based on per-particle species mass fractions and mass fraction of particles as described in detail in Riemer and West [2013].

This study focused on submicron aerosols because they are the dominant category of particles for radiation interactions and the provision of cloud condensation nuclei. We defined the mixing state indices in three different ways, namely based on chemical species abundance (χ_a), based on the mixing of absorbing and non-absorbing species (χ_o), and based on the mixing of hygroscopic and non-hygroscopic species (χ_h). The index χ_a was defined based on all the model aerosol species. A lower value for χ_a indicates that the species tend to be present in separate particles. For χ_o , we considered two surrogate species, black carbon (absorbing) and all other aerosol species grouped together (assumed to be non-absorbing). Thus, a lower value for χ_o indicates the absorbing species black carbon and the sum of all other (non-absorbing) species are more externally mixed. Similarly, χ_h was also calculated from two surrogate species. We combined black carbon, dust, and primary organic matter as one surrogate species, given their comparatively lower hygroscopicities, and salt, secondary organics, and sulfate as the other surrogate species. Correspondingly, a lower value for χ_h represents the case where hygroscopic and non-hygroscopic species tended to be present in separate particles. Note that mixing state indices defined for different purposes capture different aspects of the overall mixing state, and they are uncorrelated [Zheng et al., 2020].

2.2 Data

We used the supervised-learning surrogate models developed by Zheng et al. [2020] to predict the mixing state indices from ESM (Earth System Model) output. The surrogate models were trained on an ensemble of particle-resolved model simulations generated by the particle-resolved model PartMC-MOSAIC [Riemer et al., 2009, Zaveri et al., 2008], with the training labels for χ calculated directly from the particle-resolved data. The strategy to generate the training and testing data was to vary 45 input parameters for the PartMC-MOSAIC model scenarios, including primary emissions of different aerosol types, primary emissions of gas phase species, and meteorological parameters. A Latin Hypercube sampling approach was employed to sample the parameter space efficiently. The surrogate models were trained by using XGBoost (eXtreme Gradient Boosting, Chen and Guestrin [2016]), and can be expressed as:

$$\chi_S = f_S(A, G, E). \quad (1)$$

Where χ_S is the mixing state index (χ_a , χ_o , or χ_h) and f_S denotes the surrogate function for the corresponding mixing state index. The variants A (aerosol), G (gas), and E (environment) represent the features (variables) from the PartMC simulations that are used for predicting the mixing state index. These variables are also available from the ESM. A detailed definition of the features for the surrogate models is given in Zheng et al. [2020].

We used the simulations from the Community Earth System Model Version 2 [CESM2 version 2.1.0; Danabasoglu et al., 2020] with MAM4 [Liu et al., 2016] to provide variables at the global scale. Specifically, we used the component set “FHIST” for the global simulation configuration. This component set represents a typical historical simulation using an active atmosphere and land with prescribed sea surface temperatures and sea-ice extent, and a 1 degree finite volume dycore with the forcing data available from 1979 to 2015. We ran the model for the year 2011 with 6 years (2005-2010) spinup. The simulation was conducted at a resolution of 0.9° latitude by 1.25° longitude along with emission inventories from CMIP6 emissions [Emmons et al., 2020]. We stored the instantaneous outputs every three hours in the simulation, which yielded 2920 timestamps for each surface-layer grid cell for the entire year of simulation time.

With the surrogate models and the ESM simulation, we predicted the mixing state indices for each grid cell at each timestamp (i.e. every 3 hours). For each grid cell, the mixing state indices were averaged by month. Therefore, each grid cell has a vector of stacked mixing state indices with a length of 36 (12 months \times 3 mixing state types), represented as $\mathbf{x} = (\chi_{a,1}, \dots, \chi_{a,12}, \chi_{o,1}, \dots, \chi_{o,12}, \chi_{h,1}, \dots, \chi_{h,12})$.

2.3 Regionalization strategy

Here we interchangeably use the terms “region” and “cluster” to refer to a group of grid cells. We used the k -means unsupervised clustering algorithm to partition n grid cells into k clusters, minimizing the within-cluster variances. The k -means method has been applied to environmental sciences for ecoregion delineation [Kumar et al., 2011], environmental risk zoning of the chemical industrial area [Shi and Zeng, 2014], and clustering haze trajectory of peatland fires [Khairat et al., 2017], among other applications.

In our case, given $n = 55\,296$ (192 latitude \times 288 longitude) grid cells $(\mathbf{x}_1, \mathbf{x}_2, \dots, \mathbf{x}_{55296})$, where each grid cell contains a 36-dimensional vector (three mixing state indices over 12 months), k -means clustering aims to partition these grid cells into k ($k \leq n$) sets $\mathcal{S} = \{S_1, S_2, \dots, S_k\}$ so as to minimize the within-cluster variance. The objective is to find:

$$\arg \min_{\mathcal{S}} \sum_{i=1}^k \sum_{\mathbf{x} \in S_i} \|\mathbf{x} - \boldsymbol{\mu}_i\|^2 \quad (2)$$

where $\boldsymbol{\mu}_i$ is the mean of the points in S_i .

The k -means clustering method requires the a priori specification of the number of clusters (k). As the value of k increases, the variance V_k asymptotically approaches 0 until k equals n . Here we used the relative difference in variance between $k - 1$ and k to determine the number of clusters. Starting from $k = 2$, we computed the criteria of relative difference $V_{k-1} - V_k \leq 0.05V_{k-1}$ to determine the cluster number k . In this study, since $V_{10} - V_{11} \leq 0.05V_{10}$, we selected $k = 11$ clusters.

3 Results

The regional clusters of mixing state are shown in Figure 1. Unlike with supervised learning, the performance of unsupervised learning are challenging to evaluate since there is no ground truth. However, the clustering process of this study was merely based the information of mixing state indices, without the direct guidance such as aerosol species distribution or other explicit spatial information. Therefore a success indicator of the spatiotemporal clustering is whether spatially-contiguous regions emerge from this procedure. The clusters in Figure 1 exhibit notable regional patterns among the eleven clusters (mixing state zones), suggesting that this approach has indeed identified meaningful clusters. Each cluster has a unique spatiotemporal distribution of three mixing state indices, and captures the spatiotemporal variations that could not be detected by the global overall averages. For example, ocean regions (e.g., clusters 8, 9, 10 in the Southern Hemisphere) tend to display a more pronounced seasonal cycle than land regions (e.g., cluster 7) and overall averages.

Clusters 1 (the Arctic) and 11 (the Antarctic) were characterized by high mixing state indices (with monthly means of at least 67%) throughout the year. The high values of all three mixing state indices means that the different aerosol species are rather internally mixed in these regions. Clusters 5 (tropical oceans), 8 (the South China Sea, Indian Ocean and the Pacific Ocean in the northern hemisphere near the equator, and the northern part of the Southern Ocean) and 9 (the southern part of the Southern Ocean) were ocean areas. Similar bulk aerosol composition was predicted in these regions, however the annual cycle of mixing state varies more for clusters 8 and 9 than for 5. Clusters 2, 3, and 4 covered oceans at mid and high latitudes in the Northern Hemisphere, and lands including Northern and Southern America, Europe, Middle East, Southeast Asia, as well as Australia. Clusters 6 (the region across the Atlantic from Western and Northern Africa to the northeast coast of South Africa, as well as part of the Indian Ocean) and 7 (Middle, Eastern, and Southern Africa, as well as Asia) were characterized by their higher values in χ_o compared to χ_a and χ_h , meaning that black carbon and non-absorbing species are comparatively internally mixed.

4 Conclusions

In this paper, we developed a simple but effective unsupervised learning approach to regionalize global aerosol mixing state indices. We used the monthly averages of the spatially-varying aerosol mixing state indices as input data. Each grid cell was then assigned to a region using k -means clustering without explicit spatial information as input. This approach resulted in eleven distinct regions over the world with specific spatial aggregation patterns. Each region exhibited a unique

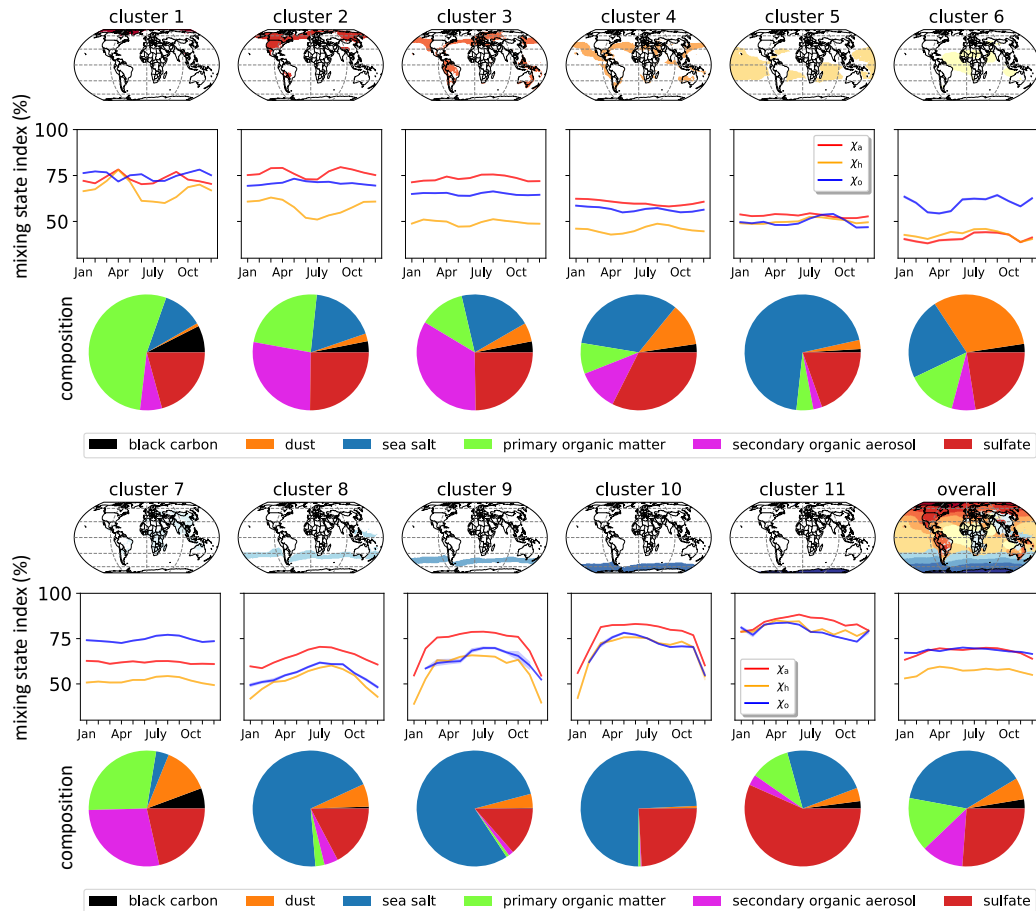


Figure 1: Aerosol mixing state zones based on unsupervised regionalization. Also shown are monthly average mixing state indices and annual averages of aerosol species mass fractions (bulk composition).

distribution of mixing state indices, suggesting that the unsupervised regionalization approach had identified meaningful regions. To the best of our knowledge, this is the first study to define aerosol mixing state zones, which we anticipate will be helpful for future studies of the global aerosol burden.

Acknowledgments and Disclosure of Funding

We would like to acknowledge high-performance computing support from Cheyenne (doi:10.5065/D6RX99HX) provided by NCAR's Computational and Information Systems Laboratory, sponsored by the National Science Foundation. The CESM project is supported primarily by the National Science Foundation. This research used resources of the Oak Ridge Leadership Computing Facility, which is a DOE Office of Science User Facility supported under Contract DE-AC05-00OR22725. This research was supported in part by an appointment to the Oak Ridge National Laboratory ASTRO Program, sponsored by the U.S. Department of Energy and administered by the Oak Ridge Institute for Science and Education. We also acknowledge funding from DOE grant DE-SC0019192 and NSF grant AGS-1254428. This research is part of the Blue Waters sustained-petascale computing project, which is supported by the National Science Foundation (awards OCI-0725070 and ACI-1238993) the State of Illinois, and as of December, 2019, the National Geospatial-Intelligence Agency. Blue Waters is a joint effort of the University of Illinois at Urbana-Champaign and its National Center for Supercomputing Applications. Louisa Emmons is thanked for thoughtful comments on the CESM2 simulations and the manuscript. We thank AWS for providing AWS Cloud Credits for Research.

References

- Amy L. Bondy, Daniel Bonanno, Ryan C. Moffet, Bingbing Wang, Alexander Laskin, and Andrew P. Ault. The diverse chemical mixing state of aerosol particles in the southeastern United States. *Atmos. Chem. Phys.*, 18(16):12595–12612, 2018. ISSN 1680-7324. doi: 10.5194/acp-18-12595-2018.
- Tianqi Chen and Carlos Guestrin. XGBoost: A Scalable Tree Boosting System. In *Proceedings of the 22nd ACM SIGKDD International Conference on Knowledge Discovery and Data Mining*, pages 785–794, San Francisco, California, USA, 2016. ACM Press. ISBN 978-1-4503-4232-2. doi: 10.1145/2939672.2939785.
- J. Ching, N. Riemer, and M. West. Impacts of black carbon mixing state on black carbon nucleation scavenging: Insights from a particle-resolved model. *J. Geophys. Res. Atmos.*, 117(D23):n/a–n/a, 2012. ISSN 01480227. doi: 10.1029/2012JD018269.
- Joseph Ching and Mizuo Kajino. Aerosol mixing state matters for particles deposition in human respiratory system. *Sci Rep*, 8(1):8864, 2018. ISSN 2045-2322. doi: 10.1038/s41598-018-27156-z.
- Joseph Ching, Jerome Fast, Matthew West, and Nicole Riemer. Metrics to quantify the importance of mixing state for CCN activity. *Atmos. Chem. Phys.*, 17(12):7445–7458, 2017. ISSN 1680-7324. doi: 10.5194/acp-17-7445-2017.
- G. Danabasoglu, J.-F. Lamarque, J. Bacmeister, D. A. Bailey, A. K. DuVivier, J. Edwards, L. K. Emmons, J. Fasullo, R. Garcia, A. Gettelman, C. Hannay, M. M. Holland, W. G. Large, P. H. Lauritzen, D. M. Lawrence, J. T. M. Lenaerts, K. Lindsay, W. H. Lipscomb, M. J. Mills, R. Neale, K. W. Oleson, B. Otto-Bliesner, A. S. Phillips, W. Sacks, S. Tilmes, L. Kampenhout, M. Vertenstein, A. Bertini, J. Dennis, C. Deser, C. Fischer, B. Fox-Kemper, J. E. Kay, D. Kinnison, P. J. Kushner, V. E. Larson, M. C. Long, S. Mickelson, J. K. Moore, E. Nienhouse, L. Polvani, P. J. Rasch, and W. G. Strand. The Community Earth System Model Version 2 (CESM2). *J. Adv. Model. Earth Syst.*, 12(2), 2020. ISSN 1942-2466. doi: 10.1029/2019MS001916.
- Louisa K. Emmons, Rebecca H. Schwantes, John J. Orlando, Geoff Tyndall, Douglas Kinnison, Jean-François Lamarque, Daniel Marsh, Michael J. Mills, Simone Tilmes, Charles Bardeen, Rebecca R. Buchholz, Andrew Conley, Andrew Gettelman, Rolando Garcia, Isobel Simpson, Donald R. Blake, Simone Meinardi, and Gabrielle Pétron. The Chemistry Mechanism in the Community Earth System Model Version 2 (CESM2). *J. Adv. Model. Earth Syst.*, 12(4), 2020. ISSN 1942-2466. doi: 10.1029/2019MS001882.
- Laura Fierce, Tami C. Bond, Susanne E. Bauer, Francisco Mena, and Nicole Riemer. Black carbon absorption at the global scale is affected by particle-scale diversity in composition. *Nat Commun*, 7(1):12361, 2016. ISSN 2041-1723. doi: 10.1038/ncomms12361.
- Laura Fierce, Nicole Riemer, and Tami C. Bond. Toward Reduced Representation of Mixing State for Simulating Aerosol Effects on Climate. *Bull. Amer. Meteor. Soc.*, 98(5):971–980, 2017. ISSN 0003-0007, 1520-0477. doi: 10.1175/BAMS-D-16-0028.1.
- Robert G. Fovell and Mei-Ying C. Fovell. Climate zones of the conterminous united states defined using cluster analysis. *J. Clim.*, 6(11):2103–2135, 1993. ISSN 0894-8755. doi: 10.1175/1520-0442(1993)006<2103:CZOTCU>2.0.CO;2.
- Matthew Fraund, Don Pham, Daniel Bonanno, Tristan Harder, Bingbing Wang, Joel Brito, Suzane de Sá, Samara Carbone, Swarup China, Paulo Artaxo, Scot Martin, Christopher Pöhlker, Meinrat Andreae, Alexander Laskin, Mary Gilles, and Ryan Moffet. Elemental Mixing State of Aerosol Particles Collected in Central Amazonia during GoAmazon2014/15. *Atmosphere*, 8(12):173, 2017. ISSN 2073-4433. doi: 10.3390/atmos8090173.
- R. M. Healy, N. Riemer, J. C. Wenger, M. Murphy, M. West, L. Poulain, A. Wiedensohler, I. P. O’Connor, E. McGillicuddy, J. R. Sodeau, and G. J. Evans. Single particle diversity and mixing state measurements. *Atmos. Chem. Phys.*, 14(12):6289–6299, 2014. ISSN 1680-7324. doi: 10.5194/acp-14-6289-2014.
- H. Holmgren, K. Sellegri, M. Hervo, C. Rose, E. Freney, P. Villani, and P. Laj. Hygroscopic properties and mixing state of aerosol measured at the high-altitude site Puy de Dôme (1465 m a.s.l.), France. *Atmos. Chem. Phys.*, 14(18):9537–9554, 2014. ISSN 1680-7324. doi: 10.5194/acp-14-9537-2014.

- Michael Hughes, John Kodros, Jeffrey Pierce, Matthew West, and Nicole Riemer. Machine Learning to Predict the Global Distribution of Aerosol Mixing State Metrics. *Atmosphere*, 9(1):15, 2018. ISSN 2073-4433. doi: 10.3390/atmos9010015.
- Mark Z. Jacobson. Strong radiative heating due to the mixing state of black carbon in atmospheric aerosols. *Nature*, 409(6821):695–697, 2001. ISSN 0028-0836, 1476-4687. doi: 10.1038/35055518.
- H. Khairat, I. Sukaesih Sitanggang, and D. E. Nuryanto. Clustering Haze Trajectory of Peatland Fires in Riau Province using K-Means Algorithm. *IOP Conf. Ser.: Earth Environ. Sci.*, 58:012059, 2017. ISSN 1755-1315. doi: 10.1088/1755-1315/58/1/012059.
- Daniel A. Knopf, Peter A. Alpert, and Bingbing Wang. The Role of Organic Aerosol in Atmospheric Ice Nucleation: A Review. *ACS Earth Space Chem.*, 2(3):168–202, 2018. doi: 10.1021/acsearthspacechem.7b00120.
- D. Koch, M. Schulz, S. Kinne, C. McNaughton, J. R. Spackman, Y. Balkanski, S. Bauer, T. Bernsten, T. C. Bond, O. Boucher, M. Chin, A. Clarke, N. De Luca, F. Dentener, T. Diehl, O. Dubovik, R. Easter, D. W. Fahey, J. Feichter, D. Fillmore, S. Freitag, S. Ghan, P. Ginoux, S. Gong, L. Horowitz, T. Iversen, A. Kirkevåg, Z. Klimont, Y. Kondo, M. Krol, X. Liu, R. Miller, V. Montanaro, N. Moteki, G. Myhre, J. E. Penner, J. Perlwitz, G. Pitari, S. Reddy, L. Sahu, H. Sakamoto, G. Schuster, J. P. Schwarz, Ø. Seland, P. Stier, N. Takegawa, T. Takemura, C. Textor, J. A. van Aardenne, and Y. Zhao. Evaluation of black carbon estimations in global aerosol models. *Atmos. Chem. Phys.*, 9(22):9001–9026, 2009. ISSN 1680-7324. doi: 10.5194/acp-9-9001-2009.
- Jitendra Kumar, Richard T. Mills, Forrest M. Hoffman, and William W. Hargrove. Parallel k-Means Clustering for Quantitative Ecoregion Delineation Using Large Data Sets. *Procedia Computer Science*, 4:1602–1611, 2011. ISSN 18770509. doi: 10.1016/j.procs.2011.04.173.
- X. Liu, P.-L. Ma, H. Wang, S. Tilmes, B. Singh, R. C. Easter, S. J. Ghan, and P. J. Rasch. Description and evaluation of a new four-mode version of the Modal Aerosol Module (MAM4) within version 5.3 of the Community Atmosphere Model. *Geosci. Model Dev.*, 9(2):505–522, 2016. ISSN 1991-9603. doi: 10.5194/gmd-9-505-2016.
- Val L. Mitchell. The regionalization of climate in the western united states. *J. Appl. Meteorol.*, 15(9): 920–927, 1976. ISSN 0021-8952. doi: 10.1175/1520-0450(1976)015<0920:TROCIT>2.0.CO;2.
- Rachel E. O’Brien, Bingbing Wang, Alexander Laskin, Nicole Riemer, Matthew West, Qi Zhang, Yele Sun, Xiao-Ying Yu, Peter Alpert, Daniel A. Knopf, Mary K. Gilles, and Ryan C. Moffet. Chemical imaging of ambient aerosol particles: Observational constraints on mixing state parameterization. *J. Geophys. Res. Atmos.*, 120(18):9591–9605, 2015. ISSN 2169-897X, 2169-8996. doi: 10.1002/2015JD023480.
- N. Riemer and M. West. Quantifying aerosol mixing state with entropy and diversity measures. *Atmos. Chem. Phys.*, 13(22):11423–11439, 2013. ISSN 1680-7324. doi: 10.5194/acp-13-11423-2013.
- N. Riemer, M. West, R. A. Zaveri, and R. C. Easter. Simulating the evolution of soot mixing state with a particle-resolved aerosol model. *J. Geophys. Res. Atmos.*, 114(D9):D09202, 2009. ISSN 0148-0227. doi: 10.1029/2008JD011073.
- N. Riemer, A. P. Ault, M. West, R. L. Craig, and J. H. Curtis. Aerosol Mixing State: Measurements, Modeling, and Impacts. *Rev. Geophys.*, 57(2):187–249, 2019. ISSN 8755-1209, 1944-9208. doi: 10.1029/2018RG000615.
- Weifang Shi and Weihua Zeng. Application of k-means clustering to environmental risk zoning of the chemical industrial area. *Front. Environ. Sci. Eng.*, 8(1):117–127, 2014. ISSN 2095-2201, 2095-221X. doi: 10.1007/s11783-013-0581-5.
- J. Wang, M. J. Cubison, A. C. Aiken, J. L. Jimenez, and D. R. Collins. The importance of aerosol mixing state and size-resolved composition on CCN concentration and the variation of the importance with atmospheric aging of aerosols. *Atmos. Chem. Phys.*, 10(15):7267–7283, 2010. ISSN 1680-7324. doi: 10.5194/acp-10-7267-2010.

- Qing Ye, Peishi Gu, Hugh Z. Li, Ellis S. Robinson, Eric Lipsky, Christos Kaltsonoudis, Alex K.Y. Lee, Joshua S. Apte, Allen L. Robinson, Ryan C. Sullivan, Albert A. Presto, and Neil M. Donahue. Spatial Variability of Sources and Mixing State of Atmospheric Particles in a Metropolitan Area. *Environ. Sci. Technol.*, 52(12):6807–6815, 2018. ISSN 0013-936X. doi: 10.1021/acs.est.8b01011.
- Rahul A. Zaveri, Richard C. Easter, Jerome D. Fast, and Leonard K. Peters. Model for Simulating Aerosol Interactions and Chemistry (MOSAIC). *J. Geophys. Res. Atmos.*, 113(D13), 2008. ISSN 2156-2202. doi: 10.1029/2007JD008782.
- Zhonghua Zheng, Jeffrey H. Curtis, Yu Yao, Jessica T. Gasparik, Valentine G. Anantharaj, Lei Zhao, Matthew West, and Nicole Riemer. Estimating Submicron Aerosol Mixing State at the Global Scale with Machine Learning and Earth System Modeling. Preprint, EarthArXiv, 2020.
- Shupeng Zhu, Karine Sartelet, Yang Zhang, and Athanasios Nenes. Three-dimensional modeling of the mixing state of particles over Greater Paris: 3-D MIXING STATE MODELING. *J. Geophys. Res. Atmos.*, 121(10):5930–5947, 2016. ISSN 2169897X. doi: 10.1002/2015JD024241.